# Study on the mechanism of platinum-assisted hydrofluoric acid etching of SiC using density functional theory calculations

P. V. Bui, A. Isohashi, H. Kizaki, Y. Sano, K. Yamauchi, Y. Morikawa, and K. Inagaki

Citation: Applied Physics Letters **107**, 201601 (2015); doi: 10.1063/1.4935832
View online: http://dx.doi.org/10.1063/1.4935832
View Table of Contents: http://scitation.aip.org/content/aip/journal/apl/107/20?ver=pdfcov
Published by the AIP Publishing



# Study on the mechanism of platinum-assisted hydrofluoric acid etching of SiC using density functional theory calculations

P. V. Bui,[1] A. Isohashi,[1] H. Kizaki,[1] Y. Sano,[1] K. Yamauchi,[1,2,a)] Y. Morikawa,[1,2,b)] and K. Inagaki[1]

[1]*Department of Precision Science and Technology, Graduate School of Engineering, Osaka University, Osaka 565-0871, Japan*

[2]*Research Center for Ultra-Precision Science and Technology, Graduate School of Engineering, Osaka University, Osaka 565-0871, Japan*

(Received 28 April 2015; accepted 3 November 2015; published online 16 November 2015)

Hydrofluoric acid (HF) etching of the SiC surface assisted by Pt as a catalyst is investigated using density functional theory. Etching is initiated by the dissociative adsorption of HF on step-edge Si, forming a five-fold coordinated Si moiety as a metastable state. This is followed by breaking of the Si–C back-bond by a H-transfer process. The gross activation barrier strongly correlates with the stability of the metastable state and is reduced by the formation of Pt–O chemical bonds, leading to an enhancement of the etching reaction. © *2015 AIP Publishing LLC*.
[http://dx.doi.org/10.1063/1.4935832]

Chemical etching and cleaning are important processes in the manufacture of integrated circuits because the manufacturing yield and device performance are sensitive to surface roughness, impurities, and defects introduced at various stages of the process. One of the most widely used etching and cleaning techniques for Si, vitreous silicon dioxide ($SiO_2$), and other silicate glasses is dipping in an aqueous hydrofluoric acid (HF).[1–4] At room temperature, the oxide layer on the Si surface readily dissolves in aqueous HF solutions, via the adsorption of two reactive species, namely, HF and $HF_2^-$ with the $H^+$ on the Si surface, resulting in breakage of the siloxane bonds in the $SiO_2$ network.[2–5] After complete removal of the oxide layers by HF, the Si surface is terminated with fluorine species, causing polarization of the Si back-bonds. This allows the insertion of HF into the back-bonds of the fluorine-terminated Si, leading to the passivation of the Si surface by hydrogen.[6] Once the Si surface is passivated with hydrogen, there is no possibility of further surface attack by HF.

SiC is beginning to replace Si as the substrate material in the integrated circuits designed for high-power, high-temperature, and high-voltage applications. Understanding and controlling processes that lead to atomically flat surfaces are of crucial importance. Treating SiC surfaces with aqueous HF for removing the oxide layer is quite different from cleaning Si surfaces. Unlike the Si surface, after oxide cleaning of SiC(0001) surfaces, the topmost Si atoms are predominantly terminated with OH species, because they cannot be removed by HF.[7–12] Recently, some of the authors of the present study developed a method called catalyst-referred etching (CARE) for surface planarization,[13–17] where SiC surfaces are etched in HF solutions with a Pt catalyst. Atomically smooth SiC surfaces with a structure consisting of atomically flat terraces with one bilayer-height step were produced.[16] High-density signals of O 1s and F 1s states were detected in the XPS measurements, indicating that F and OH-terminated Si co-exist on the etched SiC surface after CARE.[14–18] Recently, Arima *et al.*[14] proposed a mechanism for SiC etching in HF with Pt catalyst using CARE. They suggested that the SiC surface is first oxidized by Pt, and the oxide layer is subsequently removed by HF. However, they did not provide a detailed explanation for the $F^-$ termination observed on the SiC surface after CARE. Additionally, the $F^-$-terminated SiC surface contradicts the argument by Dhar *et al.*,[7] who suggested that the etching of $SiO_2$ on SiC would lead to OH termination of the SiC surface.

Previously, we investigated the dissociation of HF molecules on F- and OH-terminated SiC surfaces without a Pt catalyst, using first-principles simulations and found that the energy barriers for the direct dissociation pathways are larger than those for the indirect two-step dissociation pathways. In the indirect two-step pathways, the HF molecule dissociates into H and F. F is bonded to the surface Si atom, forming a five-fold coordinated structure, whereas H is bonded to the neighboring OH moiety forming $H_2O$ in the first step, following which the H moves to break the Si–C back-bond and terminate the C dangling bond. The lowest energy barrier for this process was calculated to be 1.2 eV.[19–21] The relatively large values of barrier heights calculated are consistent with experimental results, which indicate that the SiC surface cannot be removed by HF in the absence of a Pt catalyst.

A good understanding of the CARE mechanism is crucial for its practical application in industry as a global polishing method. In this study, we therefore propose a mechanism for the breaking of the first Si–C bond via CARE by clarifying the contribution of chemical and elastic interactions between the Pt and SiC surfaces and discuss the role of Pt as a catalyst in the etching process.

A slab model containing a stepped 3C–SiC(111) surface similar to the surface structure observed after CARE and Pt(111) layers is shown in Fig. 1. In employing the 3C–SiC(111) model, consisting of four bilayers in a unit

a)Electronic mail: yamauchi@prec.eng.osaka-u.ac.jp
b)Electronic mail: morikawa@prec.eng.osaka-u.ac.jp

 

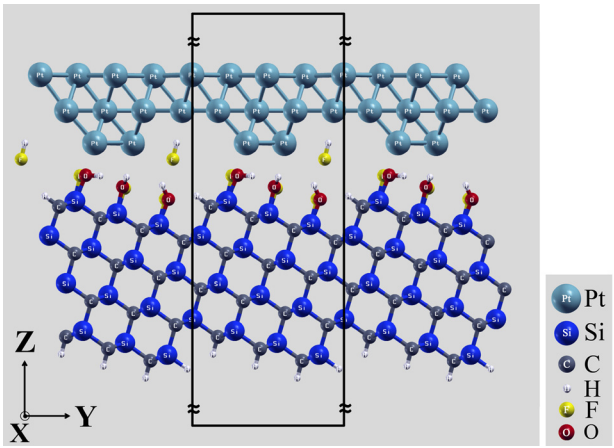


FIG. 1. A side view of the 3C–SiC (111) model with the step-and-terrace structure. The box indicates a unit cell in the calculation model.

cell, we expected the calculated adsorption energies and activation barriers to be similar to those for the 4H–SiC(0001) surfaces because of the similarities in the local atomic configurations and surface energies.[22] The Pt(111) surface was chosen because a high-intensity Pt(111) peak was observed in the X-ray diffraction pattern of deposited Pt in a previous study.[23] A stepped Pt surface was employed because of its high activity, which is ideal for identifying the low-energy reaction pathway for the hydrolysis of HF at the SiC–Pt interfaces. Successive slabs were separated by a vacuum region with a thickness of about 20 Å in a direction normal to the Pt(111) surface. C atoms at the edge of the step and dangling bonds in the bottom layers of the SiC model were terminated by H atoms. Furthermore, Si atoms in the topmost surface were terminated by Si–OH or Si–F. During the simulations, the adsorbates, the two topmost bilayers of SiC along with the terminated atoms, and the bottom layer of Pt were allowed to fully relax, while the remaining atoms were fixed in position to maintain the substrate and Pt(111) structures.

The calculations were performed by the first-principles approach using the Simulation Tool for Atom Technology (STATE) program package, which has been successfully applied for investigations on metals, semiconductors, and organic materials.[24,25] The first-principles simulations were based on the generalized gradient approximation with the Perdew-Burke-Ernzerhof functional.[26] Ion cores were replaced by Troullier-Martins type norm-conserving pseudo-potentials for the Si atoms and ultrasoft pseudo-potentials for the C, H, O, F, and Pt atoms.[27] Valence wave functions and charge densities were expanded in the plane wave basis sets with cut-off energies of 25 and 225 Ry, respectively. A $3 \times 2 \times 1$ uniform k-point mesh was used in the entire surface Brillouin zone. To calculate the reaction path, the climbing image nudged elastic band method was adopted.[28,29] Optimization was performed iteratively until the residual forces acting on all the atoms at the saddle point were reduced to below $10^{-3}E_h/a_0$, where $E_h = 27.211$ eV and $a_0 = 0.529$ Å.

To simplify the models, all the simulations were conducted at zero temperature. Any influence from $H_2O$ as a solvent was neglected. In the present study, HF was considered an etchant interacting with the SiC surface. The reaction pathway and energy barrier height during the initial stages of HF etching of the SiC surface with a Pt catalyst are presented in this paper. Activation barriers were calculated as the energy difference between the transition and initial states.

We investigated several possible pathways for the dissociation of HF on F- and OH-terminated SiC surfaces with a Pt catalyst.[18–21,34] We restricted ourselves to the indirect two-step pathways because they were found to exhibit lower barrier heights in the absence of Pt. In the presence of Pt, the calculated barrier heights were found to depend significantly on the Pt position, especially on the Pt–SiC separation and z-direction rather than on the x- or y-direction. In Fig. 2, side views of the initial state (IS), metastable state (MS), two transition states (TS), and final state (FS) are shown for the case with the lowest barrier height (hereafter denoted as z0 model). To clarify the origin of the dependence of the barrier height on Pt–SiC separation, models with two different positions of Pt, namely, z0 and z0.5, were chosen. In the z0.5 model, the Pt layer is located 0.5 $a_0$ higher along the z-direction than in the z0 model.

The first step from the IS to MS involves a HF dissociative adsorption process, where the F from HF is dissociatively adsorbed on the targeted Si atom, while the H from HF is absorbed on the Pt layer. Subsequently, a five-fold coordinated Si moiety is formed in the MS. In the second step, involving the transition of the MS to FS, the H belonging to OH, which is the terminal group on the Si surface, is transferred to the C of the Si–C back-bond, leading to breaking of the Si–C bond. In the z0 model, the least distances between Pt and terminal O in the IS, MS, and FS are calculated as 2.28 Å, 2.15 Å, and 2.03 Å, respectively. The Pt–O bond lengths calculated for the MS and FS are consistent with the previously reported low-energy electron diffraction analysis results and the calculation results[30] for $\mathrm{Pt}(111) - (\sqrt{3} \times \sqrt{3})\mathrm{R30}^\circ - 2\mathrm{OH}$. The activation barriers of the z0 and z0.5 models are 0.8 and 1.1 eV, respectively, as shown in Fig. 3.

The destabilization of the MS and FS in the Pt–SiC separation is clearly seen in Fig. 3. The energy differences between the MS and IS in the z0.5 and z0 models are 0.19 eV and −0.05 eV, respectively, whereas the differences between the FS and IS in the z0.5 and z0 models are 0.1 and −0.1 eV, respectively. Moreover, the corresponding values for MS and FS with IS in the no-Pt model[19] are 0.4 and 0.05 eV. The lower barrier height is mainly due to the stabilization of the MS.

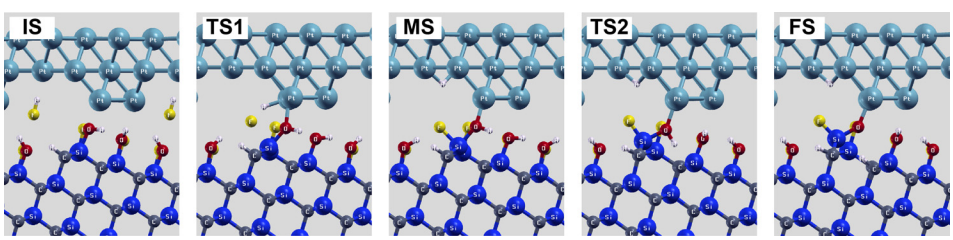


FIG. 2. Side views of the initial state (IS), transition state 1 (TS1), metastable state (MS), transition state 2 (TS2), and final state (FS) of the z0 model.

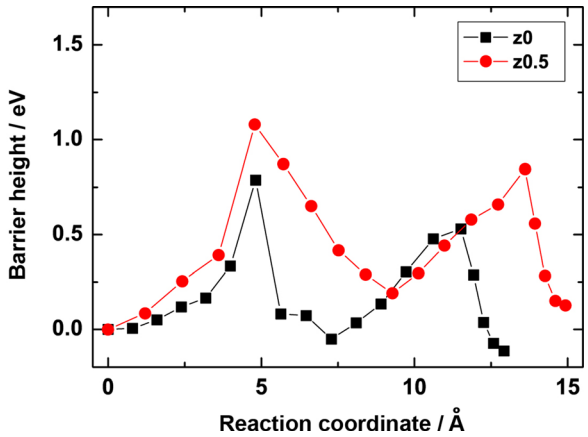


FIG. 3. Reaction energy profile for the dissociative adsorption of the first HF molecule onto an OH–terminated step-edge Si atom in the z0 and z0.5 models.

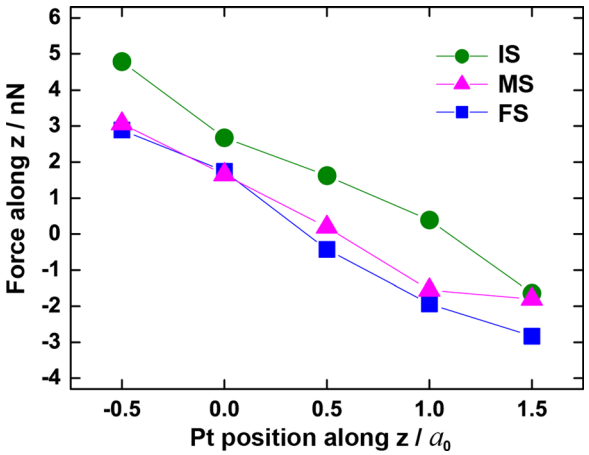


FIG. 5. Forces applied on the Pt(111) layer at the IS, MS, and FS when the Pt surface is moved toward the SiC surface along the z-direction.

Figure 4 shows the dependence of total energies at the IS, MS, and FS as a function of Pt–SiC separation. The z $\infty$ model is defined as a combination of the no-Pt model[19] and bare Pt layer. When Pt moves away from the SiC surface, the reaction pathway is expected to shift to the no-Pt model. The IS energy is destabilized below z = 1.5 $a_0$, while the MS and FS energies are stabilized and exhibit minimum values at z = 0.5 $a_0$. Furthermore, the three values come close to each other at around z = 0 $a_0$. Therefore, the activation barrier between the IS and MS should be reduced with a decrease in the Pt–SiC separation from 1.5 to 0 $a_0$.

Figure 5 shows the force exerted on the Pt layer along the z-direction as a function of the Pt–SiC separation. The force at the z0 model is about 2 nN, which is comparable with the mean value of the force between the probing tip and sample in an atomic force microscope operated in non-contact mode.[31,32] Therefore, the forces exerted on the Pt and SiC at z0 model are not too large to damage the surfaces. Moreover, the barrier height in the z0 model is quite low, so we conclude that z = 0 $a_0$ is the most appropriate position for etching at room temperature.

To clarify the origin for the dependence of the barrier heights on the Pt–SiC separation, the energy differences between the z0 and z1.5 models in the IS, MS, and FS are compared (Fig. 6). The interaction energy between the Pt and SiC surfaces are considered to contain two contributions, namely, elastic energy and chemical energy. Elastic energy is related to the deformation or distortion of atoms at the SiC–Pt interface. The differences in the elastic energies ($\Delta E^x_{elas}$) between the z0 and z1.5 models for the IS, MS, and FS are calculated by

$$\Delta E^x_{elas} = [E^x_{Pt(z0)} - E^x_{Pt(z1.5)}] + [E^x_{SiC(z0)} - E^x_{SiC(z1.5)}], \quad (1)$$

where $E^x_{Pt}$ and $E^x_{SiC}$ are the energies of the separated Pt and SiC models, with their geometries fixed to those of the $x$ states, where $x$ = IS, MS, or FS. Furthermore, the difference in chemical energy ($\Delta E^x_{chem}$) is related to the bond formation between the surface Pt and terminal O, and is calculated as

$$\Delta E^x_{chem} = E^x_{Tot} - \Delta E^x_{elas}, \quad (2)$$

where $E^x_{Tot}$ is the total energy in the $x$ state ($x$ = IS, MS, or FS).

A positive energy difference implies that the z0 model is less stable than the z1.5 model, and vice versa. At the IS and FS, elastic energy differences are the main contributors to the total energy differences. In contrast, in the MS, chemical energy plays a key role because of the Pt–O bond formation. To confirm the Pt–O bond formation, we calculated the density of states (DOS) of the two models in the MS. The DOS of the terminal O ($p_z$ orbital), the Pt ($d_{zz}$ orbital) bonded with the terminal O, the total DOS of the targeted Si, C back-

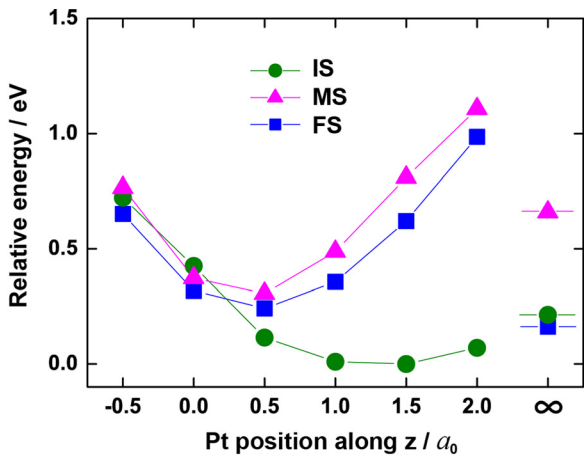


FIG. 4. Relative energies at IS, MS, and FS when the stepped Pt(111) surfaces are moved toward the SiC surfaces along the z-direction.

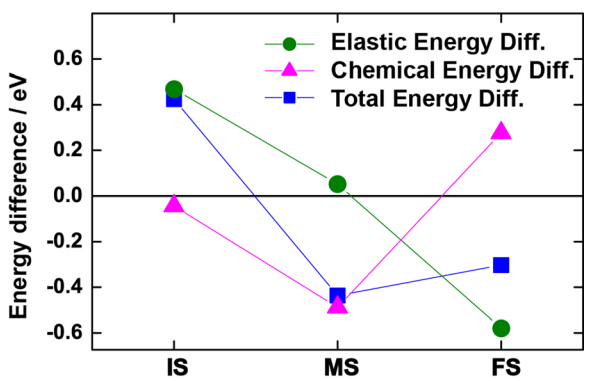


FIG. 6. Contributions of energy differences between the z0 and z1.5 models.

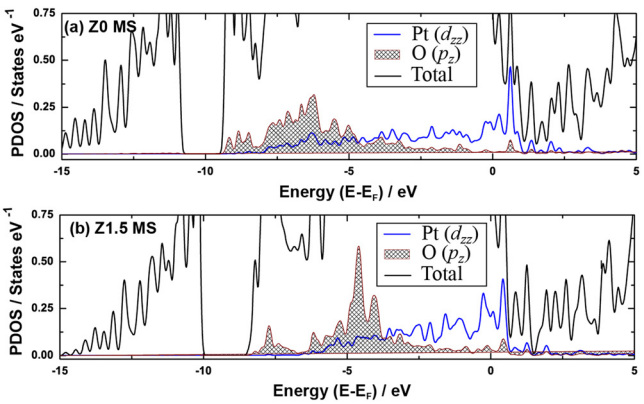


FIG. 7. DOS of Pt $d_{zz}$, O $p_z$ and the total DOS in the MS for (a) z0 and (b) z1.5 models. These DOS are aligned along the vertical direction for easy comparison.

bond, the Pt, and the terminal O at the MS of the z0 and z1.5 models are shown in Fig. 7.

The most significant difference in the DOS between the z0 and z1.5 models appears in the bonding and anti-bonding states of Pt–O, to which O $p_z$ and Pt $d_{zz}$ orbitals mainly contribute. The total DOS of all the atoms in the z1.5 model is shifted to higher energies than those in the z0 model, owing to the formation of dipoles[33] at the SiC–Pt interfaces. The bonding state of Pt–O in the z1.5 model appears from −5 to −4 eV (shaded area in Fig. 7(b)) and the anti-bonding state appears from −2 to +0.5 eV. In the case of the z0 model, the corresponding states appear at around −8 to −5 eV (shaded area of Fig. 7(a)) and −1 to +1 eV, respectively, indicating the enhanced splitting between the two states due to shorter Pt–O distance. Lowering of the DOS of bonding states and shifting up of anti-bonding states above the Fermi level associated with the MS due to the Pt–O bond formation is important for the promotion of the catalytic reaction.

The results from the density functional simulations clarified the origin of the enhancement for the etching of SiC in HF with Pt as a catalyst. HF molecules dissociate and adsorb on the Si atoms at the step-edge, forming five-fold coordinated Si moieties. In particular, the formation of Pt–O bonds in the MS and FS stabilize the SiC–Pt system, leading to a lowering of the barrier height for the etching of SiC in HF. After the Si–C back-bond breaking, the H adsorbed on the Pt surface is transferred to the terminal O, forming OH termination on the targeted Si again, leading to both F and OH terminations at the targeted Si.[34] The whole catalytic cycle is being investigated by our group. We expect that the mechanism for the removal of Si from the surface in the subsequent steps will be similar to that of the breakage of the first bond investigated in this study.

This work was partially supported by funds from the Global COE Program (Center of Excellence for Atomically Controlled Fabrication Technology) and the Program of Quantum Engineering Design Course (QEDC) from the Ministry of Education, Culture, Sports, Science and Technology (MEXT). This work was also partly supported by JSPS Grant-in-Aid for Scientific Research on Innovative Areas "3D Active-Site Science": Grant No. 26105010. Numerical calculations were carried out in the computer centers at the Institute for Solid State Physics, Tohoku University, and Osaka University.

[1]R. Q. Zhang, Y. L. Zhao, and B. K. Teo, Phys. Rev. B **69**, 125319 (2004).
[2]G. A. C. M. Spierings, J. Mater. Sci. **28**, 6261 (1993).
[3]D. M. Knotter, J. Am. Chem. Soc. **122**, 4345 (2000).
[4]W. Kern, J. Electrochem. Soc. **137**, 1887 (1990).
[5]J. K. Kang and C. B. Musgrave, J. Chem. Phys. **116**, 275 (2002).
[6]G. W. Trucks, K. Raghavachari, G. S. Higashi, and Y. J. Chabal, Phys. Rev. Lett. **65**, 504 (1990).
[7]S. Dhar, O. Seitz, M. D. Halls, S. Choi, Y. J. Chabal, and L. C. Feldman, J. Am. Chem. Soc. **131**, 16808 (2009).
[8]S. W. King, R. J. Nemanich, and R. F. Davis, J. Electrochem. Soc. **146**, 1910 (1999).
[9]V. van Elsbergen, T. U. Kampen, and W. Mönch, Surf. Sci. **365**, 443 (1996).
[10]H. Tsuchida, I. Kamata, and K. Izumi, J. Appl. Phys. **85**, 3569 (1999).
[11]U. Starke, Phys. Status Solidi B **202**, 475 (1997).
[12]N. Sieber, T. Seyller, R. Graupner, L. Ley, R. Mikalo, P. Hoffmann, D. R. Batchelor, and D. Schmeisser, Appl. Surf. Sci. **184**, 278 (2001).
[13]H. Hara, Y. Sano, H. Mimura, K. Arima, A. Kubota, K. Yagi, J. Murata, and K. Yamauchi, J. Electron. Mater. **35**, L11 (2006).
[14]K. Arima, H. Hara, J. Murata, T. Ishida, R. Okamoto, K. Yagi, Y. Sano, H. Mimura, and K. Yamauchi, Appl. Phys. Lett. **90**, 202106 (2007).
[15]K. Yagi, J. Murata, A. Kubota, Y. Sano, H. Hara, K. Arima, T. Okamoto, H. Mimura, and K. Yamauchi, Jpn. J. Appl. Phys. Part 1 **47**, 104 (2008).
[16]T. Okamoto, Y. Sano, K. Tachibana, K. Arima, A. N. Hattori, K. Yagi, J. Murata, S. Sadakuni, and K. Yamauchi, J. Nanosci. Nanotechnol. **11**, 2928 (2011).
[17]J. Murata, T. Okamoto, S. Sadakuni, A. N. Hattori, K. Yagi, Y. Sano, K. Arima, and K. Yamauchi, J. Electrochem. Soc. **159**, H417 (2012).
[18]P. V. Bui, S. Sadakuni, T. Okamoto, K. Arima, Y. Sano, and K. Yamauchi, Mater. Sci. Forum **740–742**, 510 (2013).
[19]P. V. Bui, K. Inagaki, Y. Sano, K. Yamauchi, and Y. Morikawa, Mater. Sci. Forum **778–780**, 726 (2014).
[20]P. V. Bui, K. Inagaki, Y. Sano, K. Yamauchi, and Y. Morikawa, Curr. Appl. Phys. **12**, S42 (2012).
[21]P. V. Bui, K. Inagaki, Y. Sano, K. Yamauchi, and Y. Morikawa, Key Eng. Mater. **523–524**, 173 (2012).
[22]H. Hara, Y. Morikawa, Y. Sano, and K. Yamauchi, Phys. Rev. B **79**, 153306 (2009).
[23]T. Aaltonen, M. Ritala, T. Sajavaara, J. Keinonen, and M. Leskelä, Chem. Mater. **15**, 1924 (2003).
[24]T. Hayashi, Y. Morikawa, and H. Nozoye, J. Chem. Phys. **114**, 7615 (2001).
[25]Y. Morikawa, Phys. Rev. B **63**, 033405 (2001).
[26]J. P. Perdew, K. Burke, and M. Ernzerhof, Phys. Rev. Lett. **77**, 3865 (1996).
[27]D. Vanderbilt, Phys. Rev. B **41**, 7892 (1990).
[28]G. Mills, H. Jónsson, and G. K. Schenter, Surf. Sci. **324**, 305 (1995).
[29]G. Henkelman, B. P. Uberuaga, and H. Jónsson, J. Chem. Phys. **113**, 9901 (2000).
[30]A. P. Seitsonen, Y. Zhu, K. Bedürftig, and H. Over, J. Am. Chem. Soc. **123**, 7347 (2001).
[31]A. Campbellova, M. Ondracek, P. Pou, R. Perez, P. Klapetek, and P. Jelinek, Nanotechnology **22**, 295710 (2011).
[32]Y. Sugimoto, P. Pou, M. Abe, P. Jelinek, R. Perez, S. Morita, and O. Custance, Nature **446**, 64 (2007).
[33]Y. Morikawa, K. Toyoda, I. Hamda, S. Yanagisawa, and K. Lee, Curr. Appl. Phys. **12**, S2 (2012).
[34]See supplementary material at http://dx.doi.org/10.1063/1.4935832 for detailed about reaction pathways, density of states, difference of charge density, difference of charge distribution along z-direction, proton transfer reaction.